Appl. Phys. B 53, 39–45 (1991)

Applied Physics B Photophysics and Laser Chemistry

Laser-Induced Dry Chemical Etching of Mn–Zn Ferrite in CCl_2F_2 Atmosphere

Y.-F. Lu[1], M. Takai[1], S. Nagamoto[2], and S. Namba[1]

[1] Faculty of Engineering Science and Research Center for Extreme Materials, Osaka University, Toyonaka, Osaka 560, Japan
[2] D.S. Scanner Co. Ltd., 5-3-7. Fukushima, Osaka 553, Japan

Received 15 February 1991/Accepted 6 April 1991

Abstract. Maskless etching of Mn–Zn ferrite in dichlorodifluoromethane (CCl_2F_2) by Ar^+-ion laser (514.5 nm line) irradiation has been investigated to obtain high etching rates and aspect-ratio of etched grooves. The etching reaction was found to be thermochemical. High etching rates of up to 360 μm/s, which is about one order of magnitude higher than that in a CCl_4 gas atmosphere and even higher than that in a H_3PO_4 solution, have been achieved. A maximum aspect-ratio of 6.9 was obtained.

PACS: 75.50G, 81.60

Laser-induced microfabrication, as a new fabrication method for the microstructures of semiconductors, metals, and insulators, has been widely investigated in recent years [1–4].

Like semiconductors, ceramics are another important kinds of materials in the electronic industry. For example, ferrite is used as an important material for magnetic heads in the information storage system. Our previous studies on laser-induced processing of ferrite materials provided a new method to microfabricate this material with high process-rate, high precision and low damage, in which laser-induced etching of ferrite in a CCl_4 gas atmosphere or in a H_3PO_4 aqueous solution [5–8], and laser-induced deposition of buried SiO_2 line in ferrite [9] were performed.

This paper shows a new approach to etch the ferrite material by laser irradiation in a CCl_2F_2 gas atmosphere instead of other reactive halogen compounds. Since CCl_2F_2 is chemically stable at room temperature, much safer to human body than CCl_4 [10] and does not stain the metal parts in the vacuum system, it is considered to be more suitable for the industrial applications. Furthermore, CCl_2F_2 has high vapor pressure of up to several atm. at room temperature which may promote etching reaction, whereas CCl_4 has a vapor pressure of below 100 Torr. The sample used in this study is single-crystalline ferrite, which is superior in mechanical and magnetic characteristics to conventionally used poly-crystalline ferrite. For example, single crystalline ferrite has higher magnetic susceptibility, higher wear resistance and free of grains.

The etching behavior in CCl_2F_2 is compared with those in laser-induced dry etching in CCl_4 and wet etching in a H_3PO_4 aqueous solution.

1. Experimental

The schematic diagram of the experimental system is shown in Fig. 1. The experimental system includes an Ar^+-ion laser, a convex lens, a quartz-window-containing vacuum chamber, a pumping system and an etchant gas supplying system. (100)-oriented single crystalline Mn–Zn ferrite ($MnO:ZnO:Fe_2O_3 = 31:17:52$) samples were mounted on the bottom of the vacuum chamber. The

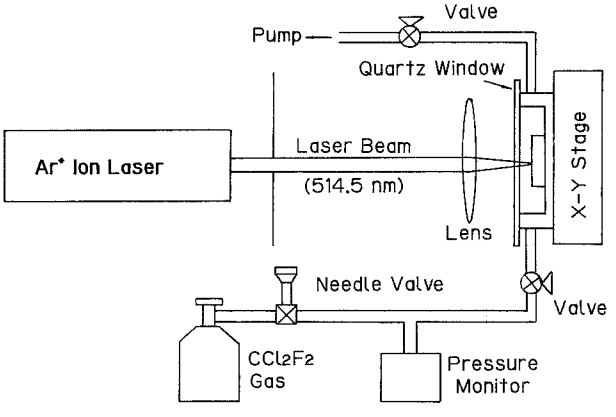

Fig. 1. Schematic diagram of the experimental system

chamber was fixed on an electronically controlled $X-Y$ stage, and evacuated by a turbomolecular pump down to 10^{-5} Torr. The ambient CCl_2F_2 gas was introduced into the chamber through a needle valve at a pressure ranging from 5 to 710 Torr. The gas pressure in the chamber was monitored by a capacitance manometer.

The 514.5 nm line of an Ar^+-ion laser was focused by a convex lens, with a focal length of 40 mm, down to a spot diameter of about 13.2 μm (at 1/e intensity) on the sample surface. The laser beam was scanned over the sample by moving the chamber with a speed ranging from 3 to 600 μm/s.

Etched patterns were observed by scanning electron microscopy (SEM) and a stylus measurement (DEKTAK) to obtain etched depth, etched width and the distribution of the reaction products of the laser-irradiated surface. Auger electron spectroscopy (AES) was used to locally investigate the atomic composition of the reaction products and the etched surface.

The etching rate was defined as the maximum etched depth divided by the beam dwell time.

2. Results and Discussion

2.1 Etching Mechanisms

Laser-induced etching of materials generally includes two steps in the reaction. The first is the dissociation of the etchant and the second is the reaction between the dissociated radicals and the substrate. According to the role of the laser beam in these two steps, the etching reaction can mainly be classified into two types: thermochemical and photochemical processes.

In the case of halogenated methanes, the photon energy necessary for the dissociation of the carbon-halogen bond depends on halogen elements: for the fluoride and chloride methane, the binding energy of carbon-halogen bond is higher than that of others. The mean binding energies for C–F bond and C–Cl bond are 117.0 Kcal/mol (5.08 eV) and 78.1 Kcal/mol (3.39 eV), respectively [11], corresponding to a photon wavelength of 244.7 and 366.7 nm. Therefore, most fluoride and chloride methanes have no absorption in the visible wavelength. For example, the mechanism of the laser-induced etching of ferrite in CCl_4 gas during laser irradiation is mainly thermochemical reaction at the sample surface [5–8, 12, 13]. From this fact, it is derived that CCl_2F_2 cannot be photochemically dissociated by the 514.5 nm line of Ar^+-ion laser.

Etching reaction does not occur on the ferrite surface in a low laser power region. The threshold laser power for laser-induced etching of ferrite in a CCl_2F_2 atmosphere in this study is found to be 0.06 W, corresponding to a local temperature rise of about 600° C [6]. This value is almost the same as the melting point of the chlorides of Fe, Mn, and Zn. Therefore, the laser-induced etching of the ferrite in CCl_2F_2 is a thermochemical process: CCl_2F_2 is thermally decomposed during laser irradiation.

Figure 2 shows the SEM cross-sectional views of the etched groove obtained with a laser power of 0.28 W, scan speed of 9 μm/s and a CCl_2F_2 pressure of 150 Torr before and after the cleaning process. The reaction products filled in the groove can be observed in Fig. 2a. These products can be easily removed by supersonic cleaning in acetone as in Fig. 2b. It has a Gaussian-shaped cross-

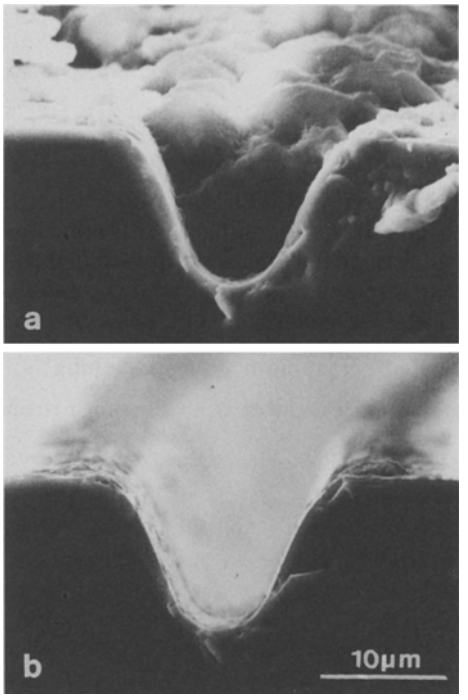

Fig. 2a, b. SEM cross-sectional views of the etched groove obtained under a condition of laser power 0.28 W, scan speed 9 μm/s and CCl_2F_2 pressure 150 Torr: (**a**) before rinse (as irradiated) and (**b**) after rinse in acetone

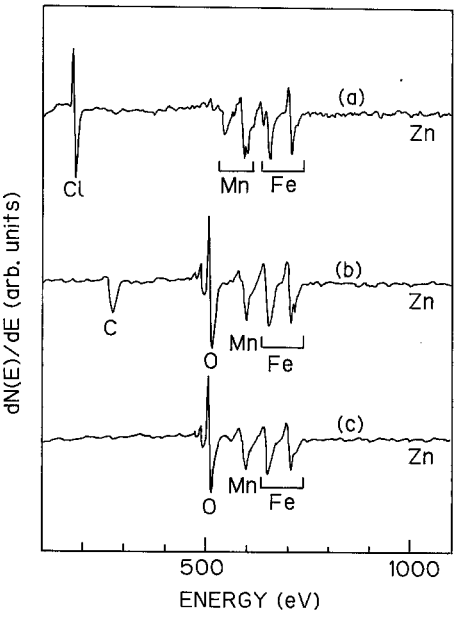

Fig. 3. AES spectra for the etched groove shown in Fig. 2: a) AES spectrum of the reaction products; b) AES spectrum of the etched surface; and c) AES spectrum of bulk ferrite for reference (after Ar^+ ion sputtering)

section and a smooth etched surface with a depth of 14 μm and a width of 18 μm.

Figure 3 shows AES spectra for ferrite samples after thermochemical etching by laser irradiation in CCl_2F_2 with the same condition as Fig. 2. In Fig. 3, (a) is the spectrum for the reaction products resided on the irradiated area, (b) is the spectrum for the surface of the etched groove after rinse in acetone, and (c) is the bulk spectrum of ferrite for a reference. The spectrum (a) of the reaction products shows Mn, Fe, Zn, and Cl peaks. No detectable peaks for C, O or F were observed in this study. The reaction products include mainly the chlorides of Mn, Fe, and Zn. Since the binding energy of C–Cl bond is much lower than that of C–F bond [11], Cl radicals are more easily decomposed thermally from CCl_2F_2 etchant gas than F radicals during laser irradiation. Therefore, the etching reaction seems mainly caused by the Cl radicals. Furthermore, the absence of oxygen signals in the products implies that etching is mainly a chemical reaction (i.e., chlorination and the vaporization of the chlorides). The spectrum (b) for the etched surface shows C peak besides the constituent elements of ferrite Mn, Zn, Fe, and O. No Cl peak was detected because all of the metal chlorides are solved in acetone and can be removed during supersonic cleaning. Sputter cleaning for 20 s by Ar ions, corresponding to a removal of 10 nm, resulted in stoichiometric ferrite without any other contamination (c).

2.2 CCl_2F_2 *Gas Pressure Dependence*

Figure 4 shows the SEM cross-sectional views of the etched grooves in a CCl_2F_2 atmosphere with different pressures. The laser power and scan speed were 0.28 W and 9 μm/s, respectively. Figure 4a shows the cross-section of the groove etched in a vacuum, indicating cracks around the groove. In this case, the etching process is due to the vaporization by the high local temperature rise induced by laser irradiation. Since the thermal conductivity and thermal diffusivity of the ferrite are much lower than those of semicondcutors, and the thermal expansion coefficient of ferrite (1.2×10^{-5}/°C) is an order of magnitude higher than that of semiconductors [6], the thermal stress due to the local temperature rise is very high and cracks are easily induced during the etching process in vacuum [5, 6]. When a CCl_2F_2 gas was introduced, a deep Gaussian-shaped groove can be obtained without cracks (Fig. 4b). The existence of the etchant gas induces thermochemical reaction at a temperature near the melting point of the metal chlorides before the local temperature reaches the melting point of the ferrite material which is much higher. Therefore, the etchant gas has two main contributions in the etching process, one is to increase the etching rate, and another is to reduce the local temperature rise. As the CCl_2F_2 pressure increases, the etching rate increases and a deep groove can be obtained with a smooth etched surface (Fig. 4c).

Figure 5 shows the etched depth and width as a function of gas pressure from 5 to 710 Torr. The laser

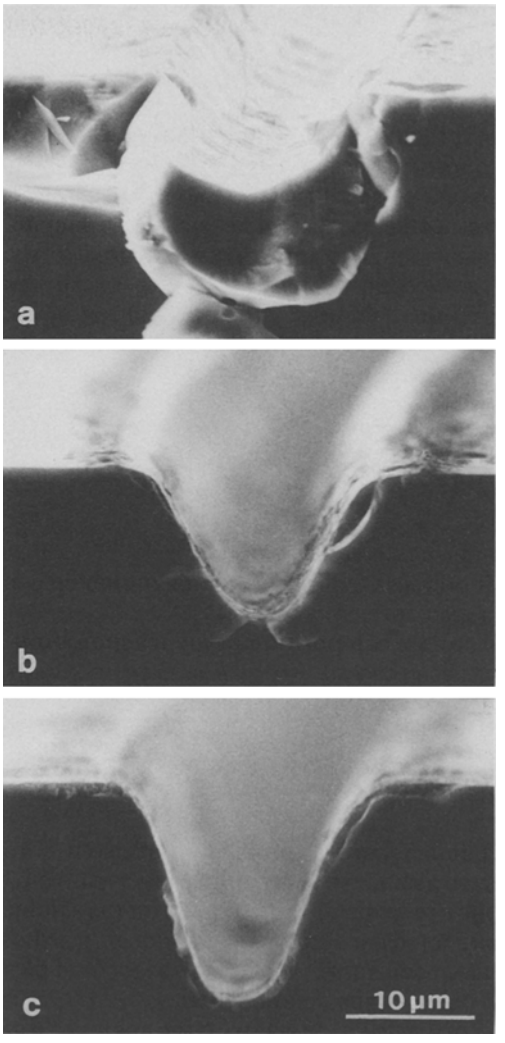

Fig. 4a–c. SEM cross-sectional views of the etched grooves obtained in different CCl_2F_2 gas pressures: (**a**) in a vacuum, (**b**) 40 Torr, and (**c**) 300 Torr with a laser power of 0.28 W and a scan speed of 9 μm/s

power and scan speed were 0.28 W and 9 μm/s, respectively. The etched depth increased logarithmically with the gas pressure without saturation from 4 to 20 μm though the etched width remained almost the same. The etching rate increased by about five times as the gas pressure ranged from 5 to 710 Torr.

Figure 6 shows the AES spectra for the reaction products at etchant gas pressures from 5 to 710 Torr. The spectra change with the pressures especially in the low pressure region. At 5 and 20 Torr, Cl, C, and O peaks can be observed besides the metal peaks of Mn, Fe, and Zn. Under these conditions, the O peak was very strong. The O peak became weaker and C peak disappeared as the CCl_2F_2 pressure was increased to 40 and 60 Torr. When the CCl_2F_2 pressure was above 80 Torr, neither O peak nor C peak can be detected. In the low pressure CCl_2F_2 ambient, the etching rate by laser irradiation is very low and only a very thin deposit layer exists on the ferrite surface, thus the peaks in AES spectra arise from the O of bulk ferrite and C of surface contamination as well as the

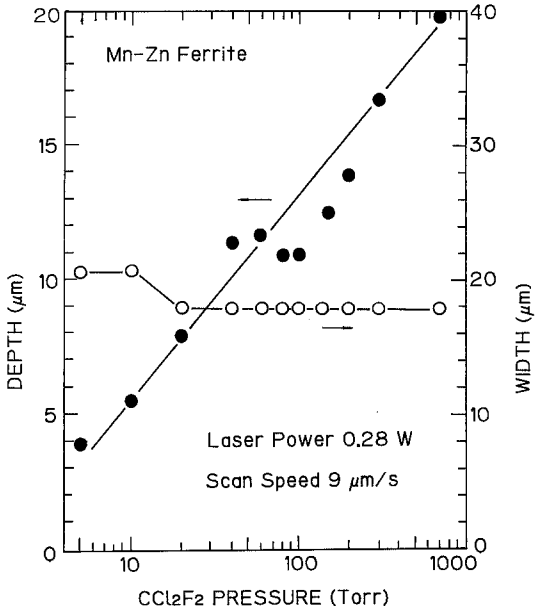

Fig. 5. CCl_2F_2 gas pressure dependence of the depth (●) and the width (○) of the etched grooves with a laser power of 0.28 W and a scan speed of 9 μm/s

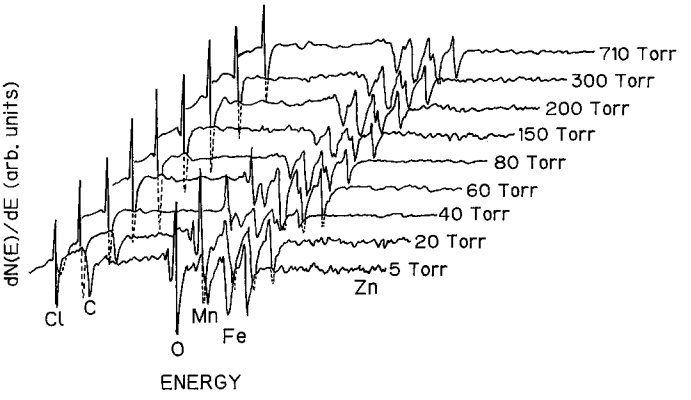

Fig. 6. AES spectra of the residual reaction products in etched grooves obtained in different CCl_2F_2 gas pressures

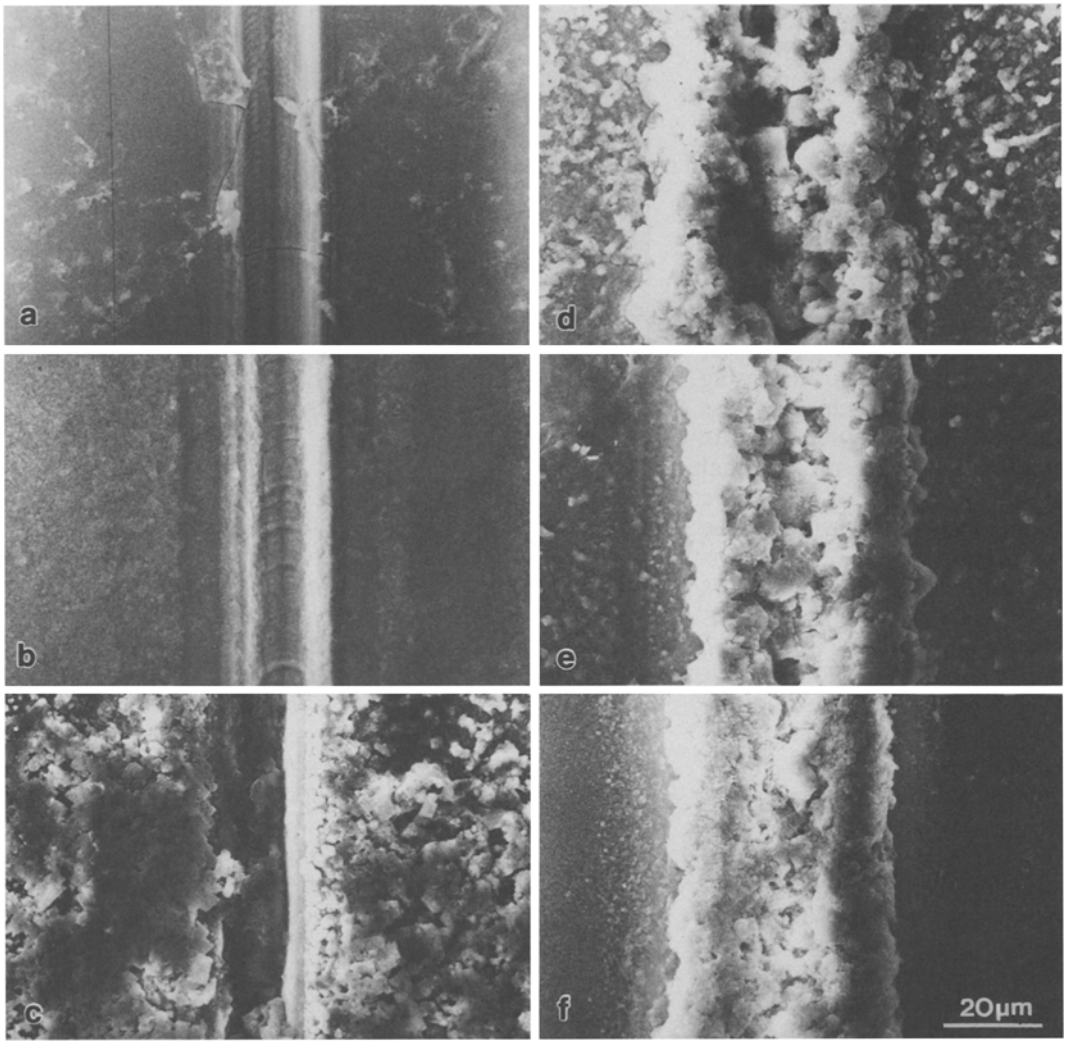

Fig. 7. Distribution of the residual products on sample surfaces in different etchant gas pressures, with a laser power of 0.28 W and a scan speed of 9 μm/s

peaks of metal chlorides for the reaction products. As the gas pressure increases, the etching rate becomes higher and then a thicker deposit layer can be formed. Therefore, the C and O peaks become weak as the gas pressure increases. When the gas pressure reaches 80 Torr and above, the deposit layer becomes thick enough so that only peaks for metal chlorides can be detected.

The distribution of the residual products (i.e., the deposits) is also an important parameter to affect the process quality in the microfabrication application: the residual deposits sometimes affect the process precision in other part on the same substrate. Figure 7 shows the distribution of the deposits obtained in CCl_2F_2 gas with a pressure ranging from vacuum to 710 Torr. The top view of the groove etched in a vacuum is shown in Fig. 7a. Cracks at and nearby the groove due to the high thermal stress induced by laser irradiation can be observed. Introduction of 10 Torr CCl_2F_2 into the vacuum chamber induced the chemical reaction in the irradiated area and avoided the formation of the cracks (Fig. 7b). When the pressure of the CCl_2F_2 gas increased to 60 Torr, a layer of deposit was formed around the irradiated area with a wide range (Fig. 7c). Although they can be removed easily by supersonic cleaning in acetone, the deposits would affect the processing of the other part of the same substrate. However, when the gas pressure became higher, the products started to concentrate in the center of the irradiated area (Fig. 7d–f). This phenomenon is considered to be due to the drastic change in mean free path of the product diffusion during the etching process with pressure change of about three orders of magnitude.

2.3 Laser Power and Scan Speed Dependences

Figure 8 shows the SEM cross-sectional views of the etched grooves obtained with laser powers of 0.19, 0.47, and 0.75 W. The scan speed and CCl_2F_2 gas pressure were 9 μm/s and 700 Torr, respectively. When the laser power is low, a typical Gaussian shaped groove can be obtained (Fig. 8a). As the laser power increased, the groove became deeper though the width did not increase much (Fig. 8b). As the laser power reached 0.75 W, a very deep groove with a high aspect-ratio was obtained (Fig. 8c). The depth, width and aspect-ratio are 172, 25, and 6.9 μm, respectively. The measured focus depth of the lens is about 30 μm, much smaller than the groove depth. The incoming beam would, therefore, be confined inside the wall, which prevents the beam from diverging, and the beam propagates to the reacting layer by light guiding, which is caused by the high surface reflectivity on the side walls due to the large incident angle of the laser beam [7].

Figure 9 shows the etched depth and width as a function of laser power from 0.2 to 0.8 W, with a scan speed of 9 μm/s and a gas pressure of 700 Torr. The etched depth increased exponentially with laser power without saturation, and the etched width remained almost unchanged though the laser power changed from 0.2 to 0.8 W. These results are considered to be due to the low thermal conductivity of ferrite which confines heat in the region at and nearby the irradiated area.

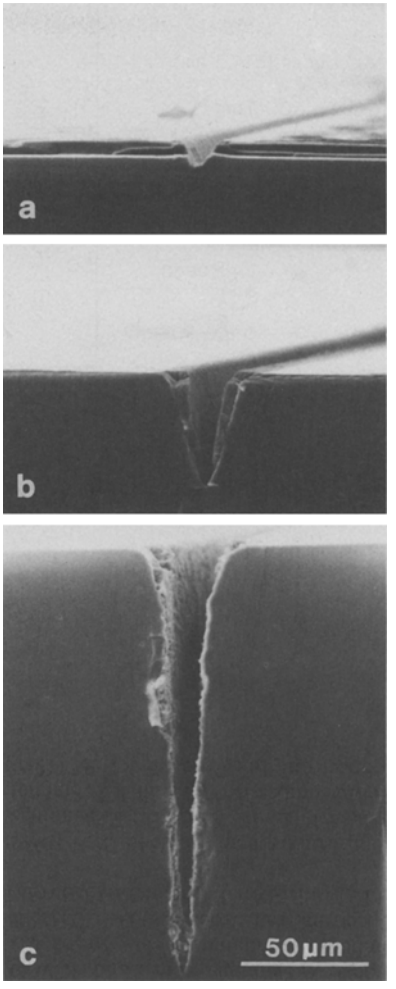

Fig. 8a–c. SEM cross-sectional views of the etched grooves with different laser powers: (**a**) 0.19 W, (**b**) 0.47 W and (**c**) 0.75 W, with a scan speed of 9 μm/s and a CCl_2F_2 gas pressure of 700 Torr

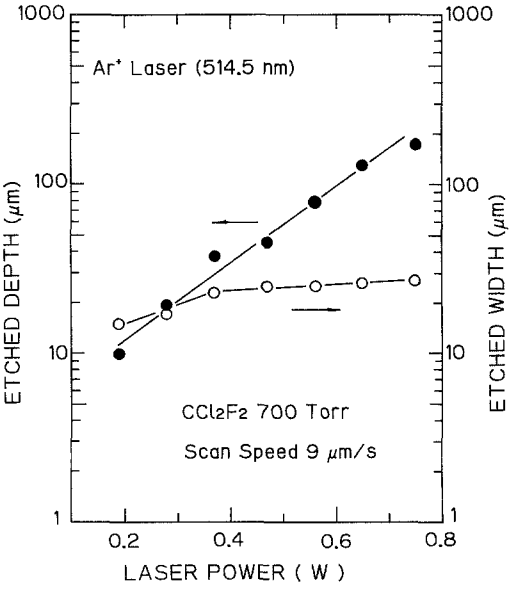

Fig. 9. Laser power dependence of the depth (●) and the width (○) of the etched grooves with a CCl_2F_2 pressure of 700 Torr and a scan speed of 9 μm/s

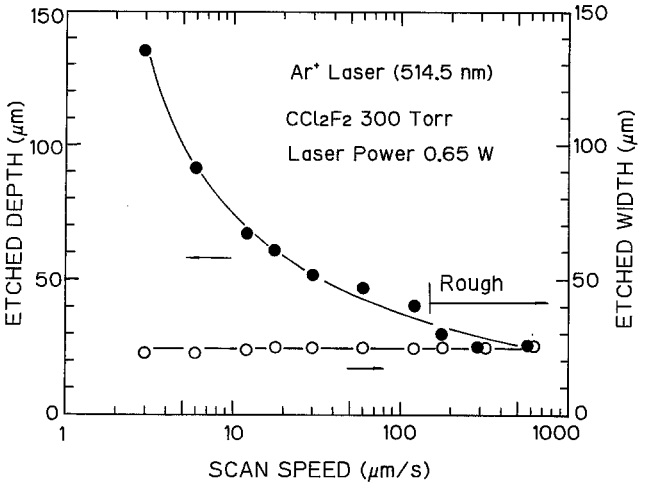

Fig. 10. Scan speed dependence of the depth (●) and the width (○) of the etched grooves with a laser power of 0.28 W and a CCl_2F_2 gas pressure of 300 Torr

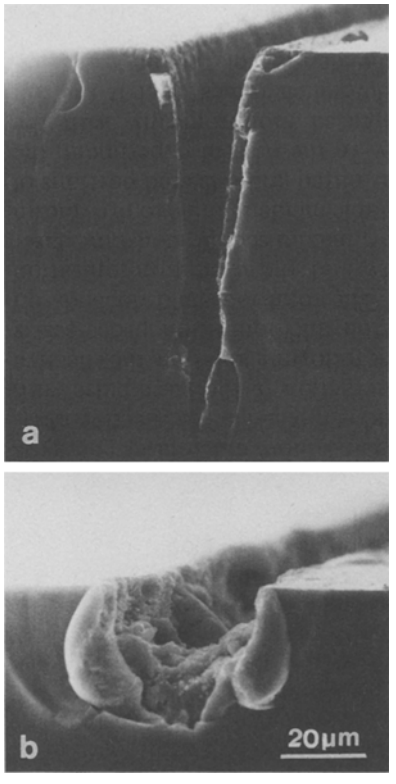

Fig. 11a, b. SEM cross-sectional views of the etched grooves with different scan speeds: (**a**) 6 μm/s and (**b**) 180 μm/s, with a laser power of 0.65 W and a CCl_2F_2 gas pressure of 300 Torr

Figure 10 shows the etched depth and width as a function of scan speed from 3 to 600 μm/s with a gas pressure of 300 Torr and a laser power of 0.65 W. Though the etched depth decreased from 135 to 25 μm, the etched width remained unchanged. This is because that the groove width is defined by the temperature profile which depends little on the scan speed within the range used in this study [6]. When the scan speed became higher than 180 μm/s, the etched groove became very rough because of the drastic change in the temperature [6]. The maximum scan speed to obtain a groove with a smooth surface is 120 μm/s. The etched depth obtained in this scan speed is 40 μm with a laser power of 0.65 W and a CCl_2F_2 pressure of 300 Torr. This etched depth corresponds to an etching rate of 360 μm/s. This value is about one order of magnitude higher than that obtained in laser-induced etching in CCl_4 gas [6] and about six orders of magnitude higher than that achieved by conventional wet-chemical etching with H_3PO_4 at room temperature (0.33 nm/s [7]). It is even higher than that obtained in laser-induced wet-chemical etching in H_3PO_4 solution [7].

Figure 11 shows the SEM cross-sectional views of two etched grooves obtained with a scan speed of 6 and 180 μm/s. The shape of the etched surface quite different because of the different scan speed. The etched groove is very deep and the etched surface is relatively smooth (Fig. 11a) at low scan speed, while the etched depth decreased and the etched surface was very rough at high scan speed. High scan speed causes high thermal stress because of the fast change in the temperature.

3. Conclusions

Laser-induced dry-chemical etching of single crystalline Mn–Zn ferrite in CCl_2F_2 was investigated. High etching rates of up to 360 μm/s and high aspect-ratios of up to 6.9 can be achieved. This etching rate is about one order of magnitude higher than that obtained in laser-induced etching in a CCl_4 gas atmosphere, and slightly higher than that obtained in laser-induced etching in a H_3PO_4 solution. The etching process is found to be thermochemical and considered to be caused by the Cl radicals thermally decomposed from the CCl_2F_2 gas. The reaction products are mainly metal chlorides and the deposits of the reaction products around the etched groove can be controlled by high etchant gas pressure and be removed by cleaning procedures after etching.

Acknowledgements. The authors are indebted to M. Matsuzawa, M. Shimizu, and H. Sandaiji of NGK Insulators, Ltd. for supplying single crystalline ferrite samples. The authors would like to thank K. Mino and K. Kawasaki for their skillfull technical assistance during this study. Invaluable discussion by Y. Yuba and A. Kinomura is greatly appreciated.

References

1. R.M. Osgood, Jr., S.R.J. Brueck, H.R. Schlossberg (eds.): *Laser Diagnostics and Photochemical Processing for Semiconductors* (North-Holland, Amsterdam 1983)
2. A.W. Johnson, D.J. Ehrlich, H.R. Schlossberg (eds.): *Laser-Controlled Chemical Processing of Surfaces* (North-Holland, Amsterdam 1984)
3. D. Bäuerle (ed.): *Laser Processing and Diagnostics*, Springer Ser. Chem. Phys. **39** (Springer, Berlin, Heidelberg 1984)
4. D.J. Ehrlich, J.Y. Tsao (eds.): *Laser Microfabrication – Thin Film Processes and Lithography* (Academic, San Diego 1989)

5. M. Takai, S. Nagatomo, T. Koizumi, Y.F. Lu, K. Gamo, S. Namba: In *Laser Processing and Diagnostics (II)*, ed. by D. Bäuerle, K.L. Kompa, L. Lande (Les Editions de Physique, Paris 1986) p. 57
6. M. Takai, Y.F. Lu, T. Koizumi, S. Nagatomo, S. Namba: Appl. Phys. A **46**, 197 (1988)
7. Y.F. Lu, M. Takai, S. Nagatomo, S. Namba: Appl. Phys. A **47**, 319 (1988)
8. Y.F. Lu, M. Takai, S. Nagatomo, T. Minamisono, S. Namba: Jpn. J. Appl. Phys. **28**, 2151 (1989)
9. Y.F. Lu, M. Takai, A. Kinomura, H. Sanda, S. Namba: Submitted to *Lasers in Materials Engineering*
10. CCl_2F_2: DFG MAK: 1000 ppm (4950 mg/m^3), CCl_4: DFG MAK: 10 ppm (65 mg/m^3): referenced from *Hazardous Chemicals Desk Reference:* ed. by N.I. Sax, R.J. Lewis, Sr. (Van Nostrond Reinhold, New York, Tokyo 1987), Japanese Edition p. 260 and p. 247
11. *Comprehensive Inorganic Chemistry*, Vol. 2, ed. by J.C. Bailar, Jr., H.J. Emeleus, R. Nyholm, A.F. Trotman-Dikenson (Pergamon, Oxford 1973) p. 1258
12. J. Tokuda, M. Takai, K. Gamo, S. Namba: *Inst. Phys. Conf. Ser.* **79**, 319 (IOP, Bristol 1986)
13. M. Takai, J. Tokuda, N. Nakai, K. Gamo, S. Namba: Jpn. J. Appl. Phys. **22**, L 757 (1983)